BIOCHEMISTRY
including biophysical chemistry & molecular biology

ARTICLE

pubs.acs.org/biochemistry

A Novel Intermediate in the Reaction of Seleno CYP119 with *m*-Chloroperbenzoic Acid

Santhosh Sivaramakrishnan,[†] Hugues Ouellet,[†] Jing Du,[‡] Kirsty J. McLean,[§] Katalin F. Medzihradszky,[†] John H. Dawson,[‡] Andrew W. Munro,[§] and Paul R. Ortiz de Montellano*[,†]

[†]Department of Pharmaceutical Chemistry, University of California, San Francisco, California 94158-2517, United States

[‡]Department of Chemistry and Biochemistry, University of South Carolina, Columbia, South Carolina 29208, United States

[§]Manchester Interdisciplinary Biocentre, Faculty of Life Sciences, University of Manchester, 131 Princess Street, Manchester M1 7DN, United Kingdom

Supporting Information

ABSTRACT: Cytochrome P450-mediated monooxygenation generally proceeds via a reactive ferryl intermediate coupled to a ligand radical $[Fe(IV)=O]^{+\bullet}$ termed Compound I (Cpd I). The proximal cysteine thiolate ligand is a critical determinant of the spectral and catalytic properties of P450 enzymes. To explore the effect of an increased level of donation of electrons by the proximal ligand in the P450 catalytic cycle, we recently reported successful incorporation of SeCys into the active site of CYP119, a thermophilic cytochrome P450. Here we report relevant physical properties of SeCYP119 and a detailed analysis of the reaction of SeCYP119 with *m*-chloroperbenzoic acid. Our results indicate that the selenolate anion reduces rather than stabilizes Cpd I and also protects the heme from oxidative destruction, leading to the generation of a new stable species with an absorbance maximum at 406 nm. This stable intermediate can be returned to the normal ferric state by reducing agents and thiols, in agreement with oxidative modification of the selenolate ligand itself. Thus, in the seleno protein, the oxidative damage shifts from the heme to the proximal ligand, presumably because (a) an increased level of donation of electrons more efficiently quenches reactive species such as Cpd I and (b) the protection of the thiolate ligand provided by the protein active site structure is insufficient to shield the more oxidizable selenolate ligand.

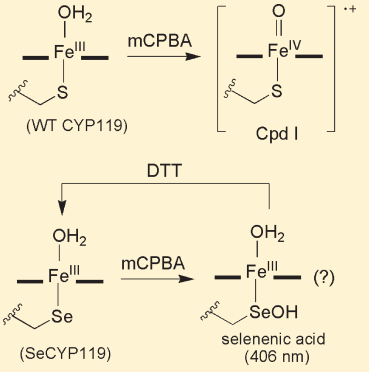

Cytochrome P450 enzymes are heme-containing monooxygenases that catalyze a variety of physiologically relevant oxidative reactions, including hydroxylation, epoxidation, and heteroatom oxidation.[1] The P450 catalytic cycle involves the generation of several intermediates, at least one of which transfers an oxygen atom to the substrate.[2] Specifically, $[Fe(IV)=O]^{+\bullet}$, a high-valent iron(IV) oxo intermediate coupled to a ligand radical, also known as Compound I (Cpd I), is thought to be the immediate species responsible for substrate oxidation.[1,2] Recent work by Green and co-workers has provided strong support for the role of this Cpd I species.[3]

The iron of the prosthetic heme in the P450 active site is coordinated on the proximal side to a cysteine thiolate ion.[4,5] This unique feature distinguishes P450 enzymes from classical peroxidases and catalases and is largely responsible for the unique spectral and catalytic properties of this class of enzymes. Earlier attempts to modulate the electron donating ability of the proximal residue in a P450 by mutating the proximal thiol to a histidine,[6,7] serine,[8] or methionine[9] resulted in the loss of both the signature spectral characteristics and catalytic activities of the P450 enzymes. These results, all of which involved less electron donating iron ligands, confirm the importance of the proximal cysteine in P450 catalysis. However, substitution of a stronger electron donor ligand has not been examined and would be potentially informative, as enhanced electron donation has been computationally predicted to both increase the rate of formation and decrease the rate of decomposition of the Cpd I intermediate.[10]

CYP119 from *Sulfolobus acidocaldarius* is a thermophilic protein that is relatively stable to both high temperature and pressure.[11] The rigid structure and remarkable physical properties of CYP119, combined with the fact that the only cysteine in its sequence is the heme iron ligand, make it an attractive system for selenocysteine substitution. Several methods for the incorporation of a selenocysteine into a protein exist.[12−14] We have successfully expressed selenocysteine-substituted CYP119, SeCYP119,[15] by expressing the protein in the presence of selenocysteine using auxotrophic BL21(DE3)CysE cells that cannot synthesize cysteine because of a mutation in their *CysE* gene.[16] Hilvert and co-workers independently reported the expression of selenocysteine-substituted CYP101A1 from *Pseudomonas putida* using an alternative approach.[17] Both of these

Received: October 27, 2010
Revised: March 4, 2011
Published: March 07, 2011

selenocysteine-substituted enzymes are stable and retain their basic spectral and catalytic properties. Specifically, SeCYP119 displays UV−vis and resonance Raman spectra that match those of the wild-type (WT) protein, confirming the presence of a six-coordinate active site heme with a water molecule as the sixth ligand. Furthermore, the catalytic activity of the seleno protein in the shunt pathway with H_2O_2 as a surrogate oxidant is comparable to that of the WT enzyme, suggesting that the proximal selenocysteine substitution preserves the overall catalytic properties of the enzyme.

Here we report physical properties of SeCYP119 relevant to its catalytic function and provide the first analysis of the reaction of any selenocysteine-substituted P450 enzyme with a surrogate oxidizing agent. Our results with *m*-chloroperbenzoic acid (*m*CPBA) and peroxynitrite (PN) as the oxidizing partners clarify the role of donation of electrons by the proximal ligand in P450 catalysis and identify a novel intermediate.

EXPERIMENTAL PROCEDURES

Materials and Methods. Buffer salts and chemicals were purchased from Fisher Scientific. L-Selenocystine and amino acids were purchased from Sigma-Aldrich (St. Louis, MO). Unless otherwise specified, all other reagents were also purchased from Sigma-Aldrich. Water was purified with a Milli-Q purification system (Millipore). All buffers and supplements were prepared using Millipore water, and the supplements were filter sterilized using a 0.22 μm filter. Auxotrophic BL21-(DE3)CysE cells were kindly provided by M.-P. Strub (National Institutes of Health, Bethesda, MD). The cells were made competent by a typical RbCl method and tested for their inability to grow in the absence of added cysteine, in both LB and minimal medium plates. HiPrep Q-FF and HisTrap Ni-NTA prepacked columns were purchased from GE Healthcare. The SeCYP119 protein was expressed and purified according to the previously reported protocol,[15] except that chloramphenicol (10 mg/L) was added to the culture (at an OD_{600} of 1.2) and incubated for a further 10 min at 37 °C immediately before the cells were washed. This method resulted in more than 80% replacement of cysteine with selenocysteine. The concentration of SeCYP119 was determined from its CO difference spectrum using an $\varepsilon_{456-490}$ of 91 mM^{-1} cm^{-1}.

All UV−vis spectrophotometric measurements were taken on a CARY 1E UV−vis spectrophotometer (Varian Inc.). The concentrations of *m*CPBA used in the assays were standardized using a triiodide assay (ε_{353} = 25.5 mM^{-1} cm^{-1}).[18] All oxidation reactions were conducted using a freshly prepared *m*CPBA stock in acetone. Peroxynitrite (PN) was prepared according to a published procedure,[19] and the concentration was determined by UV−vis spectroscopy (ε_{302} = 1670 M^{-1} cm^{-1}). The PN was aliquoted and stored at −80 °C until it was used. The alkaline pyridine hemochromogen assay was conducted as described previously.[20] Rapid mixing experiments were performed using an SF-61 DX2 double-mixing stopped-flow system (Hi-Tech Scientific, Bradford-on-Avon, U.K.) equipped with a photodiode array detector. All reactions were conducted at 10 °C unless reported otherwise. The kinetic data were analyzed using Pro-K (Applied Photophysics).

MCD spectra were recorded at a magnetic field strength of 1.41 T with a JASCO J815 spectropolarimeter equipped with a JASCO MCD-1B electromagnet and interfaced with a Silicon Solutions personal computer through a JASCO IF-815-2 interface unit. UV−visible (UV−vis) spectra were recorded using a Cary 400 spectrophotometer interfaced with a Dell personal computer. All spectral measurements were taken in 50 mM potassium phosphate buffer (pH 7.4) at 4 °C using a 0.2 cm cuvette (protein concentration of ~25 μM). Acquisition and manipulation of data with Cary or JASCO software have previously been described.[21] UV−vis spectra were recorded before and after MCD measurements to verify sample integrity. Reduction of the heme complexes was achieved via addition of a small amount of solid or a few microliters of a concentrated (25 mg/mL) sodium dithionite solution after the protein had been degassed under N_2 in a septum-sealed cuvette.

Oxidation of SeCYP119 To Generate the P406 Species. In a typical experiment, a solution of SeCYP119 (10 μM) in potassium phosphate buffer (100 mM, pH 6.2) was treated with an equal volume of phosphate buffer containing *m*CPBA (100 μM) to yield the oxidized SeCYP119 solution (final concentrations of 5 μM SeCYP119 and 50 μM *m*CPBA) with a UV−vis absorption maximum at 406 nm.

Kinetics of the *m*CPBA-Mediated Oxidation of P450 Proteins. In a typical experiment, a solution of protein (10 μM) in potassium phosphate buffer (100 mM, pH 6.2) was rapidly mixed with an equal volume of varying concentrations of the *m*CPBA solution in the same buffer (1.25, 2.5, 5, 10, 50, and 100 μM) at 10 °C in the stopped-flow mixing unit. The resulting reaction was followed with a diode array monitor. The reactions were conducted such that the final concentrations of *m*CPBA were 0.125, 0.25, 0.5, 1.0, 5, and 10 times the final protein concentration (5 μM). The changes in absorbance at 416 and 370 nm, corresponding to the ferric and Cpd I species, respectively, were monitored.[22]

Kinetics of the Reactions of P450 Proteins with Peroxynitrite (PN). In a typical experiment, a solution of protein (6 μM) in phosphate buffer (100 mM, pH 7.0) was rapidly mixed with an equal volume of varying concentrations of a freshly made PN solution in 10 mM NaOH (1, 1.5, 2, 3, and 4 mM) at 10 °C in the stopped-flow instrument (final concentrations of 3 μM enzyme and 0.5, 0.75, 1, 1.5, and 2 mM PN). The spectrum was scanned from 300 to 700 nm using a diode-array monitor. Changes in absorbance at 416 and 430 nm corresponding to the ferric and Cpd II species were monitored.[23]

Testing for the Presence of Covalent Heme Modifications. The P406 species generated at room temperature (24 °C) was injected onto a C4 column in the HPLC system and eluted using a previously reported method[24] with water (0.1% TFA) and acetonitrile (0.1% TFA) as the solvents. The eluant was monitored at 280 and 400 nm for the protein and heme, respectively.

Determination of the Catalytic Activity of P406 by the Peroxide Shunt Pathway. In a typical assay, SeCYP119 (1.2 μM) was preincubated for 5 min with *m*CPBA (12 μM) in potassium phosphate buffer (50 mM, pH 7.4). To this was added lauric acid (100 μM), and the resulting mixture was incubated either at room temperature (23 °C) or at 50 °C for 40 min (final volume, 250 μL). Alternatively, excess *m*CPBA (100 μM) or hydrogen peroxide (10 mM) was added to the reaction mixture after the addition of lauric acid to facilitate the oxidation, and the resulting mixture was then incubated as described above. The reactions were worked up, derivatized, and analyzed on a GC−MS instrument as reported previously.[15]

Trypsin Digestion and Mass Spectrometric Analysis of P406. WT and SeCYP119 proteins (~450 pmol) were oxidized under anaerobic conditions (anaerobic chamber) with a 10 equiv excess of *m*CPBA. Formation of the P406 species during the

oxidation of SeCYP119 was confirmed by UV−vis spectroscopy. The resulting mixture was incubated for 5 min, and the excess *m*CPBA was removed with a spin column (10K molecular weight cutoff, Amicon ultracentrifugal device, Millipore). The protein was then reconstituted in ammonium bicarbonate buffer (25 mM) and alkylated using iodoacetamide (10 mM) in the dark for 30 min at 24 °C. The samples were denatured with guanidine hydrochloride (final concentration, 4 M); another aliquot of alkylating agent was added, and the resulting mixtures were incubated for a further 1 h in the dark. Excess iodoacetamide was quenched with DTT (20 mM in NH_4HCO_3), and the reaction mixtures were diluted with ammonium bicarbonate (500 μL). The samples were then taken out of the glovebox and digested with trypsin (2.5 μg in NH_4HCO_3) at 37 °C overnight, concentrated in the speed vac to a final volume of 50 μL, and analyzed by LC−MS/MS using a linear ion-trap FT-ICR hybrid tandem mass spectrometer (LTQ-FT, Thermo Fisher Scientific, Bremen, Germany), measuring the precursor masses with high resolution and high mass accuracy in the magnet while performing the CID experiments in the linear trap.

Redox Potentiometry. SeCYP119 redox titrations were performed in a Belle Technology glovebox under a nitrogen atmosphere, as described previously.[25] SeCYP119 [~5 μM in 5 mL of 100 mM potassium phosphate and 10% glycerol (pH 7.0)] was titrated electrochemically using sodium dithionite as a reductant and potassium ferricyanide as an oxidant.[26] Mediators were added to facilitate electrical communication between the enzyme and electrode (2 μM phenazine methosulfate, 7 μM 2-hydroxy-1,4-naphthoquinone, 0.3 μM methyl viologen, and 1 μM benzyl viologen, to mediate in the range from 100 to −480 mV).[27] Spectra (250−800 nm) were recorded using a Cary UV-50 Bio UV−visible scanning spectrophotometer. The electrochemical potential of the solution was measured using a Mettler Toledo SevenEasy meter coupled to a Pt/Calomel electrode (ThermoRussell Ltd.) at 25 °C. The electrode was calibrated using the Fe^{3+}/Fe^{2+}-EDTA couple as a standard (108 mV). A factor of 244 mV was used to correct relative to the standard hydrogen electrode. Redox titrations were performed in both reductive and oxidative directions to ensure that the redox processes were fully reversible and hysteretic effects were not observed. There was a clear biphasic dependence of heme absorption change versus applied potential, and data were fitted to a two-electron Nernst function (eq 1, using Origin, OriginLab, Northampton, MA) to derive midpoint reduction potential data for the SeCYP119 heme iron Fe^{3+}-to-Fe^{2+} transition.

$$\text{Abs} = \frac{a \times 10^{E - E_1/59} + b + c \times 10^{E_2 - E/59}}{1 + 10^{E - E_1/59} + 10^{E_2 - E/59}} \qquad (1)$$

where Abs is the observed absorbance value at applied potential E, a is the absorbance of the fully oxidized (ferric) heme, b is the absorbance upon completion of the reduction of the first heme species, and c is the absorbance upon reduction of the second heme species. E_1 and E_2 are the corresponding midpoint potentials for these heme iron Fe^{3+}-to-Fe^{2+} transitions.

RESULTS

Thermal Stability of SeCYP119. WT CYP119 is a thermophilic enzyme that is stable up to ~80 °C.[28] To determine whether replacement of the proximal cysteine with a selenocysteine alters the thermal stability, the WT protein and SeCYP119 were preincubated in parallel at temperatures ranging from 50 to 90 °C for 60 min, after which the absorbance maximum of the ferrous−CO complex was measured by difference spectroscopy at room temperature. SeCYP119 was stable up to 70 °C with no significant heme loss but lost ~40% of its P450 content at 80 °C and >70% after incubation at 90 °C (Figure S1 of the Supporting Information). The proteins were partially precipitated upon incubation at the higher temperatures (80 and 90 °C). Overall, the thermal stability of SeCYP119 was comparable to that of WT CYP119, indicating that the active site of the seleno mutant is structurally intact even at higher temperatures.

Comparison of the MCD Spectrum of the WT and SeCYP 119 Proteins. MCD spectra of ferric and ferrous SeCYP119 were investigated to verify whether the substitution of selenocysteine (SeCys) changed the nature of the heme coordination compared to that of the WT protein. Figure S2 (Supporting Information) shows a comparison of the MCD and UV−vis absorption spectra of ferric WT and SeCYP119 proteins. The overall spectral patterns are very similar to each other, indicating the presence of a six-coordinate ferric heme with water as the sixth ligand. Similarly, addition of dithionite at 4 °C reduced the SeCYP119 slowly over 1 h to yield MCD and UV−vis spectra identical to those of the WT protein (Figure S3 of the Supporting Information), suggesting that the incorporation of SeCys has not significantly altered the heme environment.

Redox Potential of SeCYP119. Replacement of the proximal cysteine with a selenocysteine is expected to decrease the redox potential of the protein because selenium is more electron donating and has a lower redox potential than sulfur.[16,29,30] Indeed, a redox titration of SeCYP119 progressed with conversion of the ferric heme iron to the ferrous state and a concomitant shift in the Soret feature from ~416.5 to ~403 nm. In the Q-band region, the distinct α- and β-bands were lost upon reduction in favor of a merged band at ~550 nm. These spectral shifts are consistent with retention of the selenocysteine iron coordination in the reduced species.

Data fitting at a number of different wavelengths showed the process of heme iron reduction to occur in two distinct phases. These could be fitted using a two-electron Nernst function (eq 1), and analysis of the data at different wavelengths gave consistent values for the midpoint potentials [e.g., at 384 nm, $E_1 = -62 \pm 5$ mV and $E_2 = -272 \pm 3$ mV; at 403 nm (near the maximum for the ferrous heme iron), $E_1 = -67 \pm 5$ mV and $E_2 = -265 \pm 3$ mV; at 551 nm (at the Q-band maximum in the ferrous state), $E_1 = -57 \pm 5$ mV and $E_2 = -266 \pm 3$ mV]. The data indicate a heterogeneous population of heme centers in SeCYP119 and showed that the ferrous enzyme could be reoxidized to the ferric form without hysteresis in the dependence of the optical spectrum on the applied potential (Figure S4 of the Supporting Information).

Kinetics of *m*CPBA-Mediated Oxidation of SeCYP119. SeCYP119 was oxidized using the shunt pathway to investigate the influence of an electron-rich proximal SeCys on the kinetics of formation and decay of the Cpd I intermediate. For this purpose, we utilized *m*CPBA as the oxidant in substoichiometric and stoichiometric amounts to minimize heme bleaching and unwanted oxidative reactions, as it has been previously reported to generate Cpd I in reaction with WT CYP119.[22] Results from the rapid scan spectrum were analyzed with the A + B → C → D model in which species A and B correspond to the starting ferric form and *m*CPBA, respectively. The other species are defined on the basis of the specific reaction, as discussed below. Our results

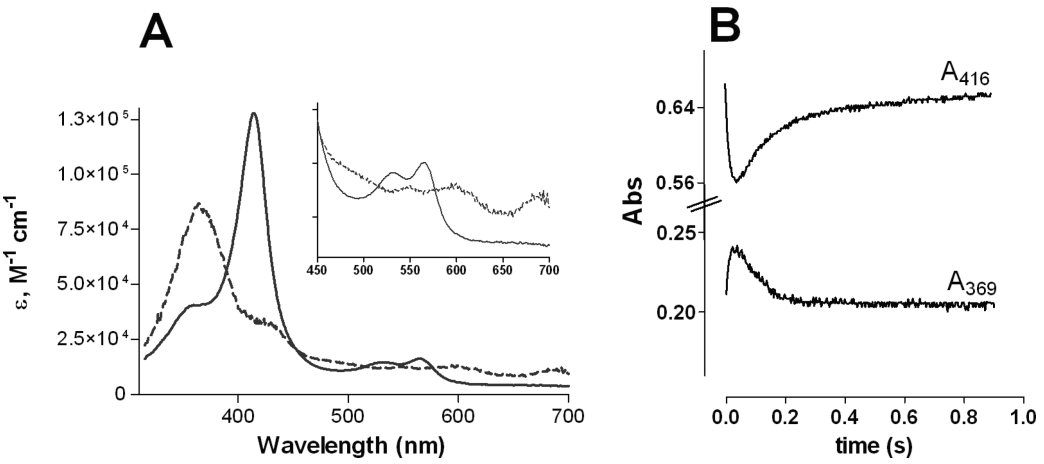

Figure 1. Spectral characterization of WT CYP119 (5 μM) upon mixing with 1 equiv of *m*CPBA (100 mM KP_i at pH 6.2 and 10 °C). (A) Calculated spectra from the SVD analysis of the rapid scan absorbance traces for the initial 0.45 s: ferric protein (—) and Cpd I (---). The inset shows a close-up of the visible region. (B) Kinetic traces of the ferric protein (416 nm) and Cpd I (369 nm).

provided no spectral evidence of accumulation of Cpd I in the *m*CPBA-mediated oxidation of SeCYP119, but a new stable species with an absorption maximum at 406 nm and a broad shoulder centered at 625 nm was observed.

Oxidation with Substoichiometric Amounts of *m*CPBA. Initially, we tested the oxidation of SeCYP119 with increasing substoichiometric concentrations of *m*CPBA [5 μM enzyme and 0.625, 1.25, and 2.5 μM *m*CPBA in 100 mM phosphate buffer (pH 6.2)] by stopped-flow spectroscopy. Interestingly, no significant changes were noticed in the rapid scan spectrum. Specifically, no increase in absorbance at 369 nm, corresponding to Cpd I, was observed (Figure S5 of the Supporting Information). SVD analysis of the rapid scan data with the A + B → C → D model revealed a species C that resembled the starting ferric protein, presumably resulting from rapid conversion of the intermediate Cpd I. Species D resembled C, but with a slight increase in the magnitude of the peak at 416 nm (Figure S5 of the Supporting Information).

Oxidation with Stoichiometric Amounts of *m*CPBA. Oxidation with 1 molar equiv of *m*CPBA [5 μM enzyme and 5 μM *m*CPBA in 100 mM phosphate buffer (pH 6.2)] resulted in significant changes in the absorbance spectra of both the WT and SeCYP119 proteins. Consistent with previous findings, the SVD analysis of the rapid scan spectrum for the oxidation of WT enzyme using the A + B → C → A model clearly showed the formation of Cpd I (species C), as characterized by its typical absorbance at 369 nm. This was followed by the rapid conversion of Cpd I back to the native ferric protein (Figure 1A). The calculated spectrum correlated well with the previously reported Cpd I spectrum of the WT enzyme.[3,22] Kinetic traces of the reaction revealed a rapid formation of the intermediate Cpd I (at 369 nm) within a few milliseconds followed by its decay. Similarly, the ferric absorbance at 416 nm decreased rapidly followed by a recovery within a few milliseconds (Figure 1B). The global analysis yielded a second-order rate constant (k_1) of 2.6×10^6 M^{-1} s^{-1} for the formation of Cpd I and a first-order rate constant (k_2) of 14.2 s^{-1} for its decay. The corresponding values determined previously at 4 °C rather than 10 °C were 4.28×10^5 M^{-1} s^{-1} and 22 s^{-1}, respectively.[22]

In contrast, accumulation of Cpd I was not observed in the oxidation of SeCYP119 with *m*CPBA under similar conditions. While very little change in the absorbance at 369 nm was observed, the Soret band shifted from 416 to 414 nm over 0.9 s. The SVD analysis of the data using the A + B → C → D model, with a k_1 of 3.4×10^6 M^{-1} s^{-1} and a k_2 of 1.1 s^{-1}, yielded a spectrum with a species C resembling the starting ferric enzyme except for a 1 nm blue shift of the Soret peak (Figure 2A). Species D showed a further blue shift of the Soret band to 414 nm along with a new broad shoulder at 625 nm and characteristic α- and β-bands at 556 and 525 nm (Figure 2A). The kinetic traces at 369 nm further indicated very little or no formation of Cpd I, while the absorbance of the 416 nm trace (ferric protein) slowly decreased over time (Figure 2B). The apparent second-order rate constant for the initial reaction of SeCYP119 with *m*CPBA (k_{app}) was comparable to that of the reaction of *m*CPBA with the WT protein. Similar results were obtained even when the oxidation was conducted at varying pH values (7.0 and 7.8). These results may suggest a highly reactive Cpd I intermediate, accompanied by a possible change in the heme environment of the SeCYP119 protein.

Oxidation with Excess *m*CPBA. We monitored the oxidation in the presence of excess *m*CPBA on the basis of the premise that increasing the rate of formation of Cpd I might help us resolve the kinetics of Cpd I formation and decay. However, the oxidation of SeCYP119 with 5 equiv of oxidant again did not give rise to the detectable formation of Cpd I. The rapid scan absorbance spectrum obtained within 0.9 s of the reaction revealed a significant shift in the ferric absorbance at 416 nm, together with a modest decrease in the absorbance of the α- and β-bands in the visible region, with no evidence of Cpd I formation (Figure 3A). However, a clear blue shift in absorbance was noticed when the reaction was monitored over 2.25 s (Figure 3A, inset) that competed with heme destruction. The SVD analysis of the data from initial 0.9 s, using the A + B → C → D model with a k_1 of 2.62×10^6 M^{-1} s^{-1} and a k_2 of 0.52 s^{-1}, revealed a species C that was identical to the untreated enzyme, but with a 2 nm shift in absorbance from 416 to 414 nm (Figure 3B). Interestingly, a new species D was observed with a Soret maximum at 406 nm. We suspected it to be a species reflecting heme loss. However, species D in SeCYP119 exhibited a 10 nm blue shift from the starting ferric spectrum with a minimal loss in the absorbance maximum at 406 nm (Figure 3B).

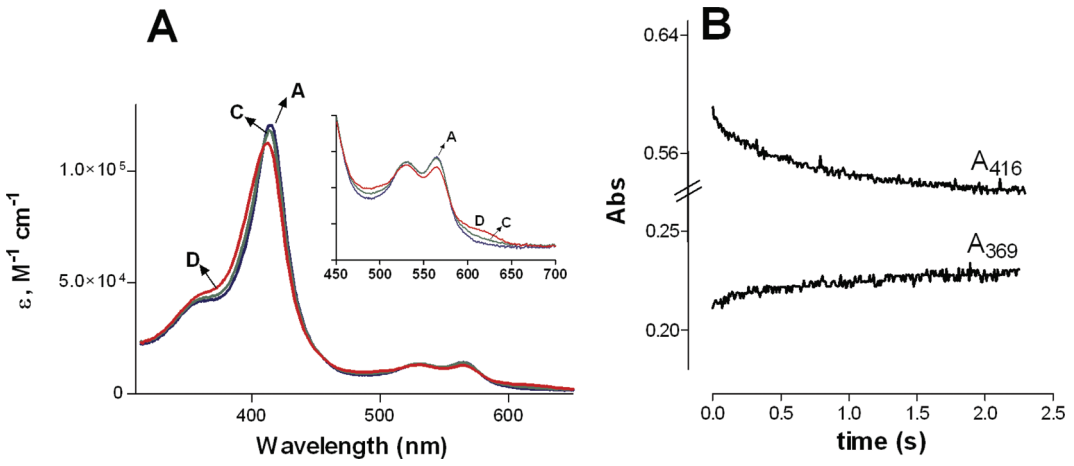

Figure 2. Spectral characterization of SeCYP119 (5 μM) upon mixing with 1 equiv of *m*CPBA (100 mM KP_i at pH 6.2 and 10 °C). (A) Calculated spectra from the SVD analysis of the rapid scan absorbance traces for the initial 0.9 s: A (ferric protein, blue), C (ferric-like protein, green), and D (ferric-like protein with a 2 nm blue shift, red). The inset shows a close-up of the visible region. (B) Kinetic traces of the ferric protein (416 nm) and Cpd I (369 nm).

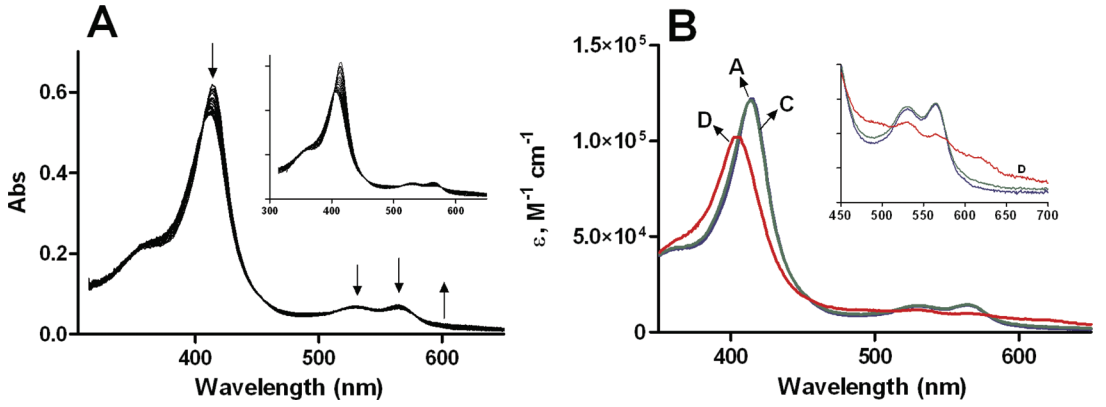

Figure 3. Spectral characterization of SeCYP119 (5 μM) upon mixing with 5 equiv of *m*CPBA (100 mM KP_i at pH 6.2 and 10 °C). (A) Traces of the rapid scan absorbance spectra obtained for the initial 0.9 s. The inset shows traces of the rapid scan spectra obtained over 2.25 s. (B) Calculated spectra from the SVD analysis of the rapid scan data of the initial 0.9 s: ferric protein (A, blue), ferric-like protein (C, green), and P406 species (D, red).

Similar results were obtained when the oxidation was conducted with a 10 equiv excess of *m*CPBA (data not shown). The final 406 nm species was stable over a period of at least 2 min under stopped-flow conditions. More importantly, the absorbance at 406 nm did not undergo a further blue shift upon addition of excess *m*CPBA but resulted in a loss of the absorbance maximum at 406 nm, consistent with possible heme destruction. Overall, increasing the expected rate of formation of Cpd I did not lead to an increase in detectable levels of Cpd I in SeCYP119. This suggests that Cpd I either is not formed or decays faster than it forms.

In an effort to observe the formation of Cpd I in SeCYP119, we oxidized the enzyme in the presence of the substrate lauric acid. The SeCYP119 was preincubated with lauric acid (50 μM) for 2 min, and the resulting solution was rapidly mixed with excess *m*CPBA in the stopped-flow instrument. No significant buildup of Cpd I was detected, as the oxidation led directly to the 406 nm species (data not shown). However, there was an ~2-fold decrease in the rate of formation of the 406 nm species, which may reflect competition between the oxidant and the lauric acid for binding within the active site.

Absence of Covalent Heme Binding. Replacement of the proximal histidine with a selenocysteine in human heme oxygenase-1 results in covalent attachment of the selenocysteine to one of the heme vinyl groups.[20] The covalently modified heme had an absorption maximum at ~402 nm.[20] We therefore investigated whether the 406 nm species, termed P406 hereafter, might represent a heme covalently attached to the protein. To test for this, the initially generated P406 was subjected to chromatography on a reverse phase C4 HPLC column with monitoring of the heme and protein at 400 and 280 nm, respectively. Normally, the prosthetic heme and the protein elute at different retention times, but in the event of covalent bond formation, the heme coelutes with the protein. In fact, the heme and protein of P406 eluted separately at 20 and 36 min, respectively (Figure S6 of the Supporting Information). Furthermore, the amount of eluted heme decreased significantly at higher *m*CPBA concentrations (from 10 to 20 equiv), consistent with more extensive oxidative heme destruction. Similar results were observed when the WT CYP119 protein was oxidized and separated by HPLC under identical conditions. Our findings establish that the prosthetic heme in P406 is not covalently attached to the protein.

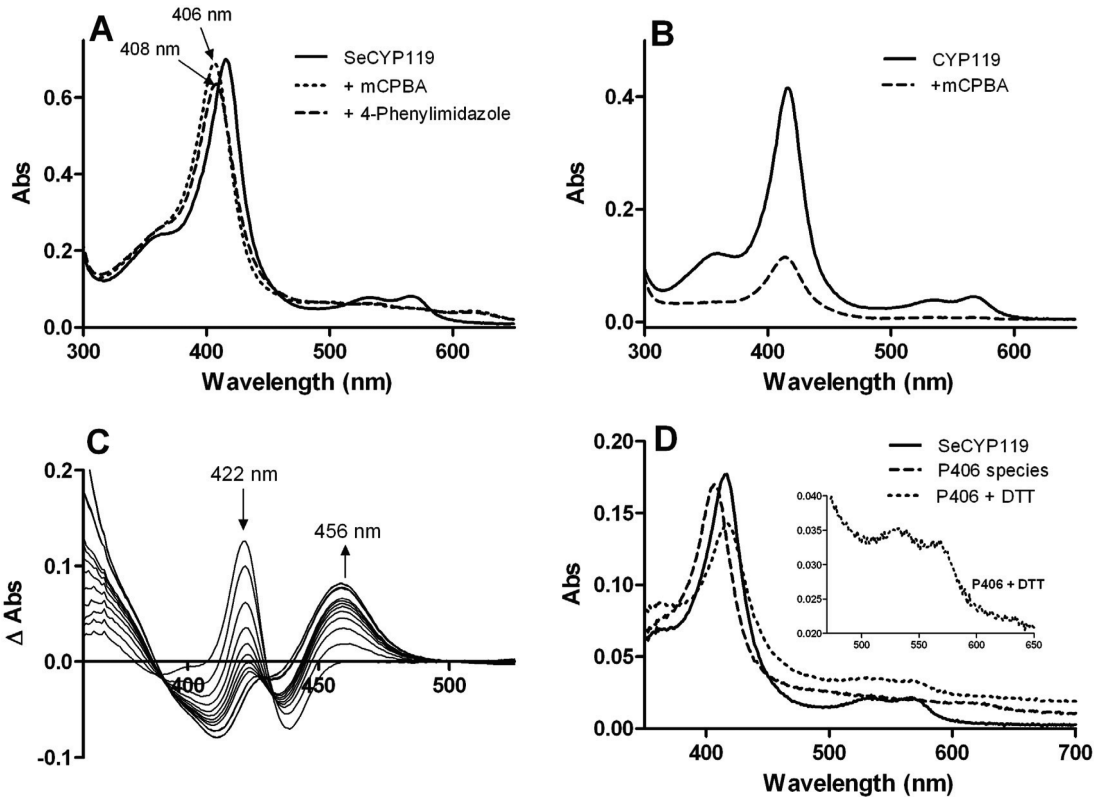

Figure 4. (A) Oxidation of SeCYP119 (5 μM) with 10 equiv of *m*CPBA (100 mM KP_i at pH 6.2 and 24 °C). Spectra are for the native protein (416 nm), the protein 5 min after the addition of 10 equiv of *m*CPBA (406 nm), and the protein 2 min after the addition of ~100 μM 4-phenylimidazole (408 nm). (B) Oxidation of WT CYP119 before and after the addition of 10 equiv of *m*CPBA. (C) Fe(II)−CO difference spectrum of the P406 species, monitored over 10 min. (D) Oxidation of SeCYP119 to generate P406 species followed by treatment with excess DTT (10 mM) to regenerate the native spectrum. The inset shows a close-up of the visible region showing the α- and β-bands of DTT-treated P406.

Catalytic Activity of P406. The ability of P406 to oxidize lauric acid was examined in the presence of excess *m*CPBA. SeCYP119 was initially oxidized to the P406 species, which was then incubated with lauric acid (100 μM) followed by the addition of excess *m*CPBA (100 μM). The reaction was allowed to proceed either at room temperature or at 50 °C, and the resulting products were extracted and analyzed by GC−MS. Interestingly, no lauric acid oxidation products were detected under these conditions (Figure S6 of the Supporting Information). However, hydroxylation of the lauric acid was observed when the enzyme was preincubated with the substrate prior to the addition of any *m*CPBA. Previously, SeCYP119 was shown to oxidize lauric acid to the ω and ω-1 hydroxylation products in the presence of excess H_2O_2.[15] Nevertheless, use of H_2O_2 (10 mM) in the P406-mediated oxidation of lauric acid under similar conditions also failed to generate the expected oxidation products. Indeed, the P406 species did not react with lauric acid, as the substrate was fully recovered after the incubation. These results indicate that P406 is not catalytically active.

UV−Vis Characteristics of P406. Given the stability of P406, it was not necessary to use stopped-flow methods for further studies. We therefore investigated the properties of this species by UV−vis spectroscopy under normal room-temperature conditions. Consistent with our expectations, P406 was formed immediately (see Materials and Methods for P406 generation) and was observed to be stable for at least 5 min at room temperature (Figure 4A). More importantly, the peak at 406 nm did not undergo a decrease in absorbance over this time period, suggesting that heme destruction was minimal. In contrast, oxidation of WT CYP119 with 10 equiv of *m*CPBA resulted in a huge decrease in the Soret maximum at 416 nm, consistent with almost quantitative heme loss (Figure 4B). Estimation of the remaining heme using the pyridine hemochromogen assay indicated a loss of no more than 40% of the total heme content upon oxidation of SeCYP119 with 10 equiv of *m*CPBA, whereas the WT enzyme lost more than 90% of its heme under the same conditions. These results suggest that SeCYP119 is much more resistant to oxidative heme loss than the WT enzyme.

We investigated the nature of the heme in P406 by adding a type II inhibitor, 4-phenylimidazole. Coordination of the nitrogen of the azole to the ferric heme iron atom should result in a red shift of the Soret band from 416 to 424 nm in the absolute spectrum.[31] Addition of 4-phenylimidazole (100−200 μM) to P406 resulted in a small 2 nm red shift in the absolute spectrum, inconsistent with the binding of a typical type II ligand to the native ferric heme (Figure 4A). We then also determined if the ferrous heme can bind carbon monoxide to yield a typical P450 spectrum. The P406 protein was flushed with carbon monoxide (Airgas) followed by the addition of sodium dithionite. A peak at 422 nm in the difference spectrum was immediately formed and then underwent complete time-dependent conversion over 5−10 min to an Fe(II)−CO complex with a maximum at 456 nm (Figure 4C). This suggests that the heme iron in P406 is in the ferric state. To determine whether molecular oxygen and/or reactive oxygen species were involved in the formation of the P406 intermediate, we conducted the *m*CPBA-mediated

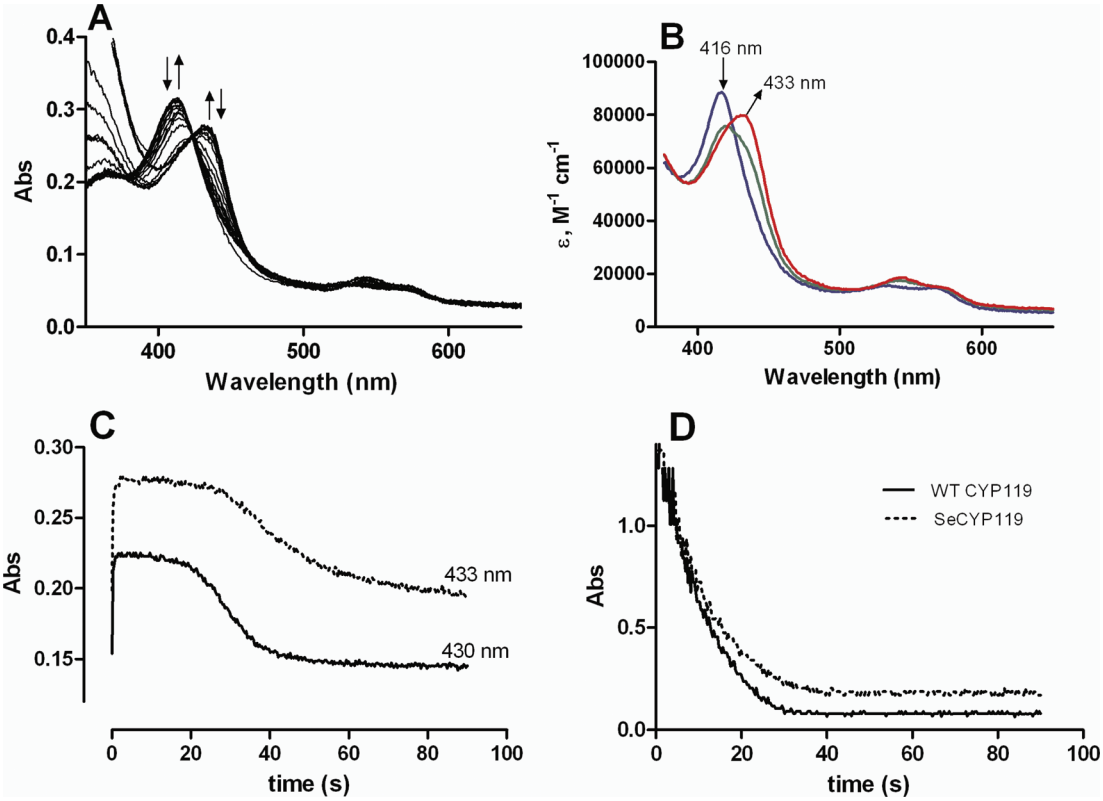

Figure 5. Oxidation of SeCYP119 with excess PN. (A) Rapid scan absorbance traces for the oxidation with 1.5 mM PN over 45 s, showing the conversion of the ferric protein (416 nm) to a Cpd II-like species (433 nm) that in turn reverts back to the starting ferric form. (B) SVD analysis of the rapid scan data for the reaction with 0.5 mM PN over 1 s, showing the formation of Cpd II: native protein (blue), SeCYP119 complex with PN (green), and Cpd II-like species (red). (C) Kinetic traces of Cpd II for the WT (430 nm) and SeCYP119 (433 nm) monitored over 90 s. (D) Kinetic traces for the PN decay over 90 s.

oxidation of SeCYP119 under strictly anaerobic conditions in a glovebox. Interestingly, P406 was generated even under anaerobic conditions, indicating that molecular oxygen is not required for its formation.

In an effort to further characterize the reversible modification that occurred in the active site, P406 generated under anaerobic conditions was denatured and reduced using DTT, followed by alkylation with iodoacetamide. The resulting protein was subjected to trypsin digestion, and the peptides were analyzed by LC−MS/MS. The active site peptide of the native SeCYP119 protein showed the expected isotopic distribution with an ion at m/z 600.9(5+) (first "visible" isotope peak) corresponding to the expected carbamidomethylated selenocysteine-containing peptide. Unfortunately, no oxidized form of the selenocysteine-containing peptide was observed upon trypsin digestion and LC−MS/MS analysis of the P406 protein. The only peptide observed was the alkylated selenocysteine-containing molecule [m/z 600.9(5+)] as in the tryptic digest of the native protein (Figure S7 of the Supporting Information). We reasoned that if SeCys had undergone an oxidative modification, it was reversed by DTT. As expected, reduction of the P406 protein in the presence of excess DTT (10 mM) resulted in an immediate red shift of the Soret maximum from 406 to 417 nm (Figure 4D). More importantly, DTT-mediated reduction led to regeneration of the signature α- and β-bands of heme, indicating the presence of a native six-coordinate ferric heme containing SeCys as its proximal ligand (Figure 4D). Furthermore, CO did not bind to the DTT-treated enzyme, indicating that the heme iron was not reduced by the DTT. However, addition of sodium dithionite resulted in the immediate generation of the conventional 456 nm spectrum.

Formation of Cpd II in the Peroxynitrite-Mediated Oxidation of SeCYP119. We investigated the reaction of PN with the SeCYP119 protein to determine whether a Cpd II species was formed. Intriguingly, oxidation of SeCYP119 with excess PN generated a species with an absorbance maximum at 433 nm. PN-mediated oxidation of chloroperoxidase is reported to generate an analogous species with an absorbance maximum at 433 nm that has been attributed to a Cpd II intermediate containing a neutral Fe(IV)−oxo species with the iron one oxidizing equivalent above the resting ferric state.[32,33] Oxidation of WT CYP119 with PN under identical conditions yielded a similar species with a maximum at 429 nm, as reported previously (data not shown).[23] Although the exact nature of this intermediate has been the subject of some controversy,[34] we will refer to our 433 nm intermediate as Cpd II on the basis of its similarity with Cpd II of chloroperoxidase.

Reaction of SeCYP119 with PN leads to a decrease in the absorbance at 416 nm of the resting ferric enzyme with a concomitant increase in the peak at 433 nm that corresponds to Cpd II (Figure 5A). The SVD analysis of the rapid scan absorbance data for the initial 1 s with the A → B → C model, fitted with a k_1 of 22 s^{-1} and a k_2 of 3 s^{-1} (at 0.5 mM PN), revealed the presence of an intermediate B that appeared to be an SeCYP119 complex with the PN, which then apparently underwent a homolytic cleavage to yield the final Cpd II species C with

an absorbance maximum at 433 nm (Figure 5B). The extent of the initial reaction of SeCYP119 with PN increased with increasing concentrations of PN, as expected for a bimolecular reaction. The apparent pseudo-first-order rate constant for the formation of Cpd II, k_2, did not exhibit any dependence on the PN concentration, consistent with a unimolecular reaction. The Cpd II intermediate was stable as long as PN was present but began to decay back to the native ferric protein once the PN was consumed. The pseudo-first-order rate constants obtained from the SVD analysis were plotted versus PN concentration to obtain the second-order rate constant for the reaction of PN with SeCYP119. Our data yield a rate constant of $(1.6 \pm 0.3) \times 10^4$ M^{-1} s^{-1} that is approximately 2.5-fold slower than that obtained for the reaction of PN with WT CYP119 under similar conditions.

Cpd II of SeCYP119 decayed more slowly than that of the WT protein to regenerate the ferric protein, as judged from their respective kinetic traces at 433 and 430 nm (Figure 5C). The stability of Cpd II depends on the concentration of PN present in the solution. Following the decay of PN at 306 nm revealed that the rate of PN consumption was comparable in both the WT and SeCYP119 reactions, with the concentration of PN approaching the baseline at around 25−30 s (Figure 5D). This suggests that the stability of Cpd II in the seleno protein is not due to the presence of excess PN. Furthermore, the species at 416 nm regenerated from Cpd II was identified as the native ferric protein by its characteristic binding to the type II inhibitor, 4-phenylimidazole. Overall, oxidation of SeCYP119 with PN led to the generation of Cpd II with a small 3 nm red shift compared to that of the WT CYP119 equivalent. More importantly, Cpd II was reduced back to the native ferric protein in a way similar to that observed for WT CYP119.

DISCUSSION

We investigated the physical properties of SeCYP119 to determine the extent to which they are altered by replacement of the proximal cysteine thiolate with a larger, more electron donating, ligand. CYP119, a thermophilic P450, is remarkably more stable than mesophilic P450 enzymes. Replacement of the active site cysteine with a selenocysteine did not alter the thermal stability of the enzyme. Some of the thermal stability of CYP119 is due to stacking interactions of aromatic residues at the protein surface,[35] but the insensitivity of the thermal stability to the selenolate for thiolate substitution is surprising. Similarly, the MCD spectra of the ferric and ferrous states of WT CYP119 and SeCYP119 exhibit no significant differences, confirming our previous conclusion from EPR and resonance Raman data that the electronic nature at the heme center in the seleno protein is very similar to that of the WT enzyme.[15] However, the redox potential of −265 mV for SeCYP119 is approximately 51 mV lower than that of WT CYP119, in accord with the redox potential difference of 48 mV between CYP101A1 and SeCYP101A1.[17] A second phase observed in the redox titration with a potential of −67 mV cannot be unambiguously assigned. This potential corresponds to a less electron donating proximal ligand and could possibly reflect the presence of some oxidized selenolate ligand. Thus, although the structural properties of CYP119 are minimally perturbed by the selenocysteine replacement, it causes a substantial change in the redox potential.

In view of the change in the redox potential, the role of the electron-rich selenocysteine ligand in the kinetics of Cpd I formation was investigated. Formation of Cpd I has been characterized by SVD analysis of the oxidation of WT CYP119 by *m*CPBA.[22] Oxidation of WT CYP119 with substoichiometric amounts of *m*CPBA generated a Cpd I intermediate with absorption maxima at 370, 610, and 690 nm.[3,22] The Cpd I spectrum was calculated from SVD analysis of the rapid scan data in which the protein underwent little reaction under limiting peracid conditions.[22] In our hands, oxidation of WT CYP119 with stoichiometric and substoichiometric concentrations of *m*CPBA produced an intermediate in the SVD analysis with spectral characteristics similar to those of the previously reported Cpd I.[3,22] Interestingly, oxidation of SeCYP119 under similar conditions did not yield a detectable Cpd I. The overall change in absorbance in the reaction of SeCYP119 with *m*CPBA was very small compared to that in the reaction of WT CYP119 under the same conditions, and the SVD analysis of the data using various kinetic models failed to generate a characteristic Cpd I intermediate. This suggests three possibilities. (a) SeCYP119 does not react with *m*CPBA. (b) The reaction occurs, but Cpd I is not formed. (c) Cpd I is formed but is very quickly reduced to the ferric state. While SeCYP119 reacted ∼3-fold less (∼6%) than the WT enzyme (∼17%), as judged by the overall change in the absorbance with 1 equiv of *m*CPBA, the amount of SeCYP119 that reacted should suffice for observation of Cpd I in the SVD analysis. Furthermore, the fact that SeCYP119 catalyzes lauric acid hydroxylation in the presence of excess H_2O_2[15] or *m*CPBA clearly suggests the formation of a Cpd I intermediate. Thus, we infer that the reaction of SeCYP119 with *m*CPBA yields an intermediate, presumably a seleno Cpd I, that is too rapidly reduced to be detected. On the basis of the SVD analysis, the apparent rate constant for the reaction of *m*CPBA with SeCYP119 was estimated to be 3.4×10^6 M^{-1} s^{-1}. However, this value has to be interpreted carefully as it may involve multiple reactions.[a] More importantly, the estimated rate constant (k_{app}) represents the slower step in the kinetics, and as Cpd I was not observed, this is presumably the initial reaction of *m*CPBA with SeCYP119. Our data indicate that *m*CPBA reacts with SeCYP119 at a rate comparable to that of the WT enzyme.

With low concentrations of the oxidant, it is possible that Cpd I decayed faster than it was formed, precluding its accumulation and spectroscopic observation. We therefore increased the rate of formation of Cpd I by increasing the concentration of the oxidant. Although these conditions cause some heme destruction, excess *m*CPBA has been used before in the oxidation of CYP101A1 to detect the formation of a Cpd I-like species.[36] However, Cpd I was not detected in the SVD analysis when SeCYP119 was oxidized with 5 or 10 equiv excesses of *m*CPBA. Our various attempts to detect the formation of Cpd I, including (a) oxidation at higher pH (pH 7.0 and 7.8), (b) using peroxyacetic acid as an alternate oxidizing agent, and (c) oxidation in the presence of lauric acid, failed to yield a detectable Cpd I intermediate. Taken together, these results argue for the formation in SeCYP119 of a Cpd I intermediate that decays faster than it forms. It is likely that the electron-rich selenolate ligand reduces Cpd I as it is formed.

Reaction of SeCYP119 with excess *m*CPBA generated a species with a Soret maximum at 406 nm (P406) that is ∼10 nm blue-shifted from the absorption maximum of the native ferric protein. Surprisingly, only 40% of the heme was lost during the oxidation of SeCYP119. Thus, SeCYP119 is much more resistant to heme destruction than the WT protein. The active site of SeCYP119 has clearly undergone an unprecedented oxidative modification that

effectively competes with the heme destruction pathway. The nature of this P406 species is discussed below.

An intermediate with an absorption maximum at 406 nm has been encountered in the *m*CPBA-mediated oxidation of CYP101A1,[37] $P450_{BM3}$,[38] and more recently CYP153A6 from *Mycobacterium* sp. HXN-1500.[39] This intermediate was assigned to Cpd ES with a neutral (or protonated) Fe(IV)=O species and a radical located on a nearby tyrosine or tryptophan residue.[40,41] Importantly, Cpd ES is relatively rapidly reduced to the native ferric state in a process that is accelerated by mild reducing agents such as ascorbic acid and guaiacol. In contrast, addition of ascorbic acid (final concentration of 1 mM) to the SeCYP119 P406 species did not alter the absorbance spectrum. Thus, although the UV−vis spectral properties of SeCYP119 P406 are similar to those observed in the reaction of *m*CPBA with CYP101A1, its stability to mild reducing agents clearly differentiates it from a Cpd ES.

Oxidation of SeCYP119 with peroxynitrite (PN) generated a Cpd II-like intermediate [neutral Fe(IV)=O species] similar to that of the WT enzyme. SeCYP119 reacts more slowly with PN than does WT CYP119, but the resulting Cpd II is more stable. Importantly, Cpd II decayed back to the native ferric protein without forming a P406 intermediate, presumably because Cpd II is not as highly oxidizing as Cpd I. The P406 intermediate thus derives from a reaction intermediate other than Cpd II.

Reduction of SeCYP119 P406 with dithionite in the presence of carbon monoxide immediately yielded a 422 nm peak in the difference spectrum that subsequently underwent complete, time-dependent conversion over 5−10 min to an Fe(II)−CO spectrum with a maximum at 456 nm identical to that of the original SeCYP119. These changes indicate that the structural features that cause the 406 nm maximum are eliminated upon reduction with sodium dithionite. On the basis of these results, we speculate that P406 has a six-coordinate low-spin ferric heme with an oxidatively modified proximal selenocysteine ligand that is reduced by dithionite back to selenocysteine. Consistent with this hypothesis, DTT, a thiol-based reducing agent, reduced the chromophore in P406 to the native ferric heme with its normal coordination and its signature α- and β-bands. Treatment with DTT apparently reduced the oxidatively modified proximal SeCys without reducing the heme iron atom. Restoration of the native protein by DTT was supported by an LC−MS/MS spectrum of the trypsin-digested P406 species that revealed an alkylated SeCys active site peptide identical to that of SeCYP119 not exposed to *m*CPBA. Taken together, these results strongly argue that P406 is a species containing an oxidatively modified active site that is completely reduced by treatment with dithionite or DTT to regenerate the native SeCYP119 protein.

It is tempting from our findings to propose oxidation of the SeCys to the selenenic acid (Se-OH), as this oxidation would be reversed by reducing agents such as dithionite and DTT. Our results rule out the presence of irreversibly oxidized forms of the proximal SeCys ligand such as SeO_2H and SeO_3H, as these should not be reduced by DTT and dithionite. Our attempts to trap a selenenic acid species using 4-chloro-7-nitrobenzo-2-oxa-1,3-diazole (NBD-Cl) have been unsuccessful. The proximal SeCys is deeply buried in the proximal side of the active site and is not readily accessible to NBD. However, we cannot rule out an intramolecular protein cross-link to form something like a selenenyl amide with the neighboring lysine residue. Thus, an alternate pathway that involves oxidation of the proximal SeCys to generate a stable two-electron oxidized species that competes with heme

Scheme 1. Proposed Pathway for the Reaction of SeCYP119 with *m*CPBA To Generate the P406 Species

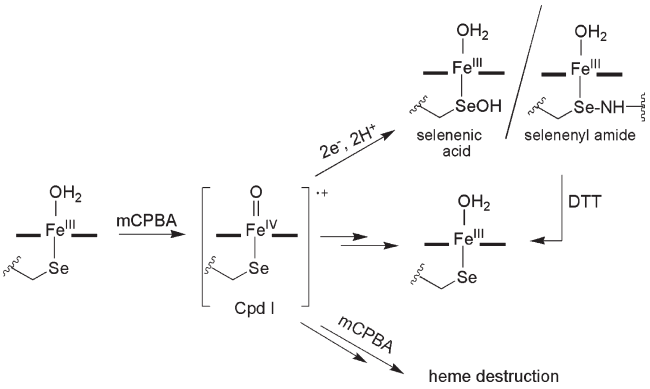

destruction is proposed (Scheme 1). The exact mechanism for this transformation is not clear at the moment. Selenols ($pK_a \sim 5.2$) are more acidic than thiols ($pK_a \sim 8.7$) and hence are deprotonated under physiological conditions.[42] In addition, the one-electron reduction potential of SeCys is approximately 0.5 V lower than that of cysteine,[43,44] and hence, SeCys should reduce Cpd I more easily than the cysteine thiolate.

Strikingly, while weaker proximal electron donors like histidine fail to support the basic spectral and catalytic properties of a P450 enzyme, a stronger electron donating selenium ligand maintains the spectroscopic characteristics but yields a less active enzyme.[15] The 2-fold lower specific activity of SeCYP119 may reflect oxidation of the selenolate ligand. MCD studies indicate that the hydrogen bonding network in the proximal cysteine pocket of CYP101A1 protects the cysteine ligand from oxidation.[45] The more acidic selenolate in SeCYP119 may disrupt this hydrogen bonding network or simply as a result of its more oxidizable nature may not be efficiently protected against oxidation by the active site environment.

In conclusion, SeCYP119 has physical properties comparable to those of WT CYP119. However, the *m*CPBA-mediated shunt pathway does not generate a detectable Cpd I under conditions that allowed its observation with the WT protein, probably because the Cpd I intermediate is rapidly reduced by the selenolate ligand. Interestingly, oxidation with excess *m*CPBA produced a stable species with an absorption maximum at 406 nm that was (a) unable to catalyze substrate oxidation when exposed to peroxides and lauric acid, (b) resistant to heme destruction, (c) unable to interact with azoles, (d) reduced to the normal, unmodified ferrous state by dithionite, and (e) reduced to the normal, unmodified ferric state by DTT. P406 is thus a novel, reversible, intermediate so far unique to SeCYP119 that may involve two-electron oxidation of the proximal selenolate ligand. The results also establish the remarkable extent to which the active site and chemistry of P450 enzymes are uniquely attuned to the thiolate ligand, with ligands of stronger or weaker electron donating ability impairing function.

■ ASSOCIATED CONTENT

Supporting Information. MCD spectra, redox potential data, rapid scan absorbance spectra, and SVD analysis for the reaction of SeCYP119 with a substoichiometric amount of

*m*CPBA (1.25 μM) and LC−MS/MS spectra of the trypsin-digested P406 species. This material is available free of charge via the Internet at http://pubs.acs.org.

AUTHOR INFORMATION

Corresponding Author

*Address: 600 16th St., University of California, San Francisco, CA 94158. Telephone: (415) 476-2903. Fax: (415) 502-4728. E-mail: ortiz@cgl.ucsf.edu.

Notes

[a]The SeCYP119 is not completely pure and contains a small amount (<20%) of the WT enzyme. However, contributions from the WT to the kinetics of Cpd I formation are negligible, because we do not observe any traces of Cpd I formation at the *m*CPBA concentrations that were used.

Funding Sources

This research was supported by National Institutes of Health Grant GM25515 (to P.R.O.d.M.) and National Center for Research Resources Grants P41RR001614 and RR019934 [to the Bio-Organic Biomedical Mass Spectrometry Resource at the University of California (director, A. L. Burlingame)].

ACKNOWLEDGMENT

We thank Mr. David Maltby at the Mass Spectrometry Facility for helpful assistance.

ABBREVIATIONS

WT, wild-type; SeCYP119, selenocysteine-substituted CYP119; P406, oxidized SeCYP119 species absorbing at 406 nm; SeCys, selenocysteine; CYP101A1 (P450cam), P450 enzyme from *Pseudomonas putida*; mCPBA, *m*-chloroperbenzoic acid; PN, peroxynitrite; DTT, dithiothreitol; GC, gas chromatography; SVD, single-value decomposition.

REFERENCES

(1) Ortiz de Montellano, P. R. (2005) *Cytochrome P450: Structure, Mechanism and Biochemistry*, 3rd ed., Kluwer Academic/Plenum Publishers, New York.

(2) Ortiz de Montellano, P. R. (2010) Hydrocarbon hydroxylation by cytochrome P450 enzymes. *Chem. Rev. 110*, 932–948.

(3) Rittle, J., and Green, M. T. (2010) Cytochrome P450 compound I: Capture, characterization, and C-H bond activation kinetics. *Science 330*, 933–937.

(4) Poulos, T. L., and Johnson, E. F. (2005) *Structures of Cytochrome P450 Enzymes*, 3rd ed., Kluwer Elsevier, New York.

(5) Dawson, J. H., and Sono, M. (1987) Cytochrome P-450 and chloroperoxidase: Thiolate-ligated heme enzymes. Spectroscopic determination of their active-site structures and mechanistic implications of thiolate ligation. *Chem. Rev. 87*, 1255–1276.

(6) Yoshioka, S., Takahashi, S., Hori, H., Ishimori, K., and Morishima, I. (2001) Proximal cysteine residue is essential for the enzymatic activities of cytochrome P450cam. *Eur. J. Biochem. 268*, 252–259.

(7) Auclair, K., Moenne-Loccoz, P., and Ortiz de Montellano, P. R. (2001) Roles of the proximal heme thiolate ligand in cytochrome $p450_{cam}$. *J. Am. Chem. Soc. 123*, 4877–4885.

(8) Vatsis, K. P., Peng, H. M., and Coon, M. J. (2002) Replacement of active-site cysteine-436 by serine converts cytochrome P450 2B4 into an NADPH oxidase with negligible monooxygenase activity. *J. Inorg. Biochem. 91*, 542–553.

(9) Murugan, R., and Mazumdar, S. (2005) Structure and redox properties of the haem centre in the C357M mutant of cytochrome P450cam. *ChemBioChem 6*, 1204–1211.

(10) Cohen, S., Kumar, D., and Shaik, S. (2006) In silico design of a mutant of cytochrome P450 containing selenocysteine. *J. Am. Chem. Soc. 128*, 2649–2653.

(11) Nishida, C. R., and Ortiz de Montellano, P. R. (2005) Thermophilic cytochrome P450 enzymes. *Biochem. Biophys. Res. Commun. 338*, 437–445.

(12) Hondal, R. J., and Raines, R. T. (2002) Semisynthesis of proteins containing selenocysteine. *Methods Enzymol. 347*, 70–83.

(13) Wu, Z. P., and Hilvert, D. (1989) Conversion of a protease into an acyl transferase: Selenolsubtilisin. *J. Am. Chem. Soc. 111*, 4513–4514.

(14) Arner, E. S., Sarioglu, H., Lottspeich, F., Holmgren, A., and Bock, A. (1999) High-level expression in *Escherichia coli* of selenocysteine-containing rat thioredoxin reductase utilizing gene fusions with engineered bacterial-type SECIS elements and co-expression with the selA, selB and selC genes. *J. Mol. Biol. 292*, 1003–1016.

(15) Jiang, Y., Sivaramakrishnan, S., Hayashi, T., Cohen, S., Moenne-Loccoz, P., Shaik, S., and Ortiz de Montellano, P. R. (2009) Calculated and experimental spin state of seleno cytochrome P450. *Angew. Chem., Int. Ed. 48*, 7193–7195.

(16) Muller, S., Senn, H., Gsell, B., Vetter, W., Baron, C., and Bock, A. (1994) The formation of diselenide bridges in proteins by incorporation of selenocysteine residues: Biosynthesis and characterization of (Se)2-thioredoxin. *Biochemistry 33*, 3404–3412.

(17) Aldag, C., Gromov, I. A., Garcia-Rubio, I., von Koenig, K., Schlichting, I., Jaun, B., and Hilvert, D. (2009) Probing the role of the proximal heme ligand in cytochrome P450cam by recombinant incorporation of selenocysteine. *Proc. Natl. Acad. Sci. U.S.A. 106*, 5481–5486.

(18) Ramette, R., and Sandford, R. W., Jr. (1965) Thermodynamics of Iodine Solubility and Triiodide Ion Formation in Water and in Deuterium Oxide. *J. Am. Chem. Soc. 87*, 5001–5005.

(19) Uppu, R. M., and Pryor, W. A. (1996) Synthesis of peroxynitrite in a two-phase system using isoamyl nitrite and hydrogen peroxide. *Anal. Biochem. 236*, 242–249.

(20) Jiang, Y., Trnka, M. J., Medzihradszky, K. F., Ouellet, H., Wang, Y., and Ortiz de Montellano, P. R. (2009) Covalent heme attachment to the protein in human heme oxygenase-1 with selenocysteine replacing the His25 proximal iron ligand. *J. Inorg. Biochem. 103*, 316–325.

(21) Huff, A. M., Change, C. K., Cooper, D. K., Smith, K. M., and Dawson, J. H. (1993) Imidazole- and alkylamine-ligated iron(II,III) chlorin complexes as models for histidine and lysine coordination to iron in dihydroporphyrin-containing proteins: Characterization with magnetic circular dichroism spectroscopy. *Inorg. Chem. 32*, 1460–1466.

(22) Kellner, D. G., Hung, S. C., Weiss, K. E., and Sligar, S. G. (2002) Kinetic characterization of compound I formation in the thermostable cytochrome P450 CYP119. *J. Biol. Chem. 277*, 9641–9644.

(23) Newcomb, M., Zhang, R., Chandrasena, R. E., Halgrimson, J. A., Horner, J. H., Makris, T. M., and Sligar, S. G. (2006) Cytochrome p450 compound I. *J. Am. Chem. Soc. 128*, 4580–4581.

(24) Meitzler, J. L., and Ortiz de Montellano, P. R. (2009) *Caenorhabditis elegans* and human dual oxidase 1 (DUOX1) "peroxidase" domains: Insights into heme binding and catalytic activity. *J. Biol. Chem. 284*, 18634–18643.

(25) Daff, S. N., Chapman, S. K., Turner, K. L., Holt, R. A., Govindaraj, S., Poulos, T. L., and Munro, A. W. (1997) Redox control of the catalytic cycle of flavocytochrome P-450 BM3. *Biochemistry 36*, 13816–13823.

(26) Dutton, P. L. (1978) Redox potentiometry: Determination of midpoint potentials of oxidation-reduction components of biological electron-transfer systems. *Methods Enzymol. 54*, 411–435.

(27) Lawson, R. J., Leys, D., Sutcliffe, M. J., Kemp, C. A., Cheesman, M. R., Smith, S. J., Clarkson, J., Smith, W. E., Haq, I., Perkins, J. B., and Munro, A. W. (2004) Thermodynamic and biophysical characterization of cytochrome P450 BioI from *Bacillus subtilis*. *Biochemistry 43*, 12410–12426.

(28) Koo, L. S., Tschirret-Guth, R. A., Straub, W. E., Moenne-Loccoz, P., Loehr, T. M., and Ortiz de Montellano, P. R. (2000) The active site of the thermophilic CYP119 from *Sulfolobus solfataricus*. *J. Biol. Chem. 275*, 14112–14123.

(29) Metanis, N., Keinan, E., and Dawson, P. E. (2006) Synthetic seleno-glutaredoxin 3 analogues are highly reducing oxidoreductases with enhanced catalytic efficiency. *J. Am. Chem. Soc. 128*, 16684–16691.

(30) Casi, G., Roelfes, G., and Hilvert, D. (2008) Selenoglutaredoxin as a glutathione peroxidase mimic. *ChemBioChem 9*, 1623–1631.

(31) Lampe, J. N., Floor, S. N., Gross, J. D., Nishida, C. R., Jiang, Y., Trnka, M. J., and Ortiz de Montellano, P. R. (2008) Ligand-induced conformational heterogeneity of cytochrome P450 CYP119 identified by 2D NMR spectroscopy with the unnatural amino acid ^{13}C-p-methoxyphenylalanine. *J. Am. Chem. Soc. 130*, 16168–16169.

(32) Nakajima, R., Yamazaki, I., and Griffin, B. W. (1985) Spectra of chloroperoxidase compounds II and III. *Biochem. Biophys. Res. Commun. 128*, 1–6.

(33) Daiber, A., Herold, S., Schoneich, C., Namgaladze, D., Peterson, J. A., and Ullrich, V. (2000) Nitration and inactivation of cytochrome P450BM-3 by peroxynitrite. Stopped-flow measurements prove ferryl intermediates. *Eur. J. Biochem. 267*, 6729–6739.

(34) Behan, R. K., Hoffart, L. M., Stone, K. L., Krebs, C., and Green, M. T. (2007) Reaction of cytochrome P450BM3 and peroxynitrite yields nitrosyl complex. *J. Am. Chem. Soc. 129*, 5855–5859.

(35) Puchkaev, A. V., Koo, L. S., and Ortiz de Montellano, P. R. (2003) Aromatic stacking as a determinant of the thermal stability of CYP119 from *Sulfolobus solfataricus*. *Arch. Biochem. Biophys. 409*, 52–58.

(36) Spolitak, T., Dawson, J. H., and Ballou, D. P. (2005) Reaction of ferric cytochrome P450cam with peracids: Kinetic characterization of intermediates on the reaction pathway. *J. Biol. Chem. 280*, 20300–20309.

(37) Spolitak, T., Dawson, J. H., and Ballou, D. P. (2006) Rapid kinetics investigations of peracid oxidation of ferric cytochrome P450cam: Nature and possible function of compound ES. *J. Inorg. Biochem. 100*, 2034–2044.

(38) Raner, G. M., Thompson, J. I., Haddy, A., Tangham, V., Bynum, N., Ramachandra Reddy, G., Ballou, D. P., and Dawson, J. H. (2006) Spectroscopic investigations of intermediates in the reaction of cytochrome P450(BM3)-F87G with surrogate oxygen atom donors. *J. Inorg. Biochem. 100*, 2045–2053.

(39) Spolitak, T., Funhoff, E. G., and Ballou, D. P. (2010) Spectroscopic studies of the oxidation of ferric CYP153A6 by peracids: Insights into P450 higher oxidation states. *Arch. Biochem. Biophys. 493*, 184–191.

(40) Schunemann, V., Jung, C., Terner, J., Trautwein, A. X., and Weiss, R. (2002) Spectroscopic studies of peroxyacetic acid reaction intermediates of cytochrome P450cam and chloroperoxidase. *J. Inorg. Biochem. 91*, 586–596.

(41) Schunemann, V., Lendzian, F., Jung, C., Contzen, J., Barra, A. L., Sligar, S. G., and Trautwein, A. X. (2004) Tyrosine radical formation in the reaction of wild type and mutant cytochrome P450cam with peroxy acids: A multifrequency EPR study of intermediates on the millisecond time scale. *J. Biol. Chem. 279*, 10919–10930.

(42) Huber, R. E., and Criddle, R. S. (1967) Comparison of the chemical properties of selenocysteine and selenocystine with their sulfur analogs. *Arch. Biochem. Biophys. 122*, 164–173.

(43) Jacob, C., Giles, G. I., Giles, N. M., and Sies, H. (2003) Sulfur and selenium: The role of oxidation state in protein structure and function. *Angew. Chem., Int. Ed. 42*, 4742–4758.

(44) Nauser, T., Dockheer, S., Kissner, R., and Koppenol, W. H. (2006) Catalysis of electron transfer by selenocysteine. *Biochemistry 45*, 6038–6043.

(45) Galinato, M. G., Spolitak, T., Ballou, D. P., and Lehnert, N. (2011) Elucidating the Role of the Proximal Cysteine Hydrogen Bonding Network in Ferric Cytochrome P450cam and corresponding mutants using Magnetic Circular Dichroism Spectroscopy. *Biochemistry 50*, 1053–1069.